Image Processing Techniques for the Quantification of Atherosclerotic Changes

K.V. Chandrinos[1], M. Pilu[2], R.B. Fisher[3], and P.E. Trahanias[1]
[1]Institute of Computer Science, Foundation for Research and Technology – Hellas (FORTH),
P.O. Box 1385, Heraklion, 711 10 Crete, Greece
[2]Digital Media Department, Hewlett-Packard Laboratories, Bristol, UK
[3]Department of Artificial Intelligence, University of Edinburgh, Scotland
e-mail: kostel@ics.forth.gr, mp@hplb.hpl.hp.com, rbf@dai.ed.ac.uk, trahania@ics.forth.gr

Abstract

This paper describes the design and implementation of an off-line, non-invasive, automated method for the examination and follow up of the arteriosclerotic changes due to hypertension, with the help of digital image processing of fundus images. This method would help in evaluating the efficacy of various treatments on the regression and reversion of arteriosclerotic lesions. This method, in interaction with appropriate knowledge bases, can be used at the clinical practice for monitoring hypertensive patients on a frequent basis, hence it aims at minimum discomfort of the patient, by-passing even the regular fluorescein injection for fundus image enhancement. Our method is based on segmenting the vasculature by identifying the centerline of each vessel utilizing the idea that vessels present a ridge in cross-sectional intensity profiles. Therefore, such a ridge can be detected along the vessels, as if there was three-dimensional information. Once the vasculature is segmented we present image-based measuring techniques for length to next bifurcation, vessel calibre, wall thickness and we introduce a novel measure of tortuosity. All our measurements are automatic, with minimal assumptions, and they are calibrated by means of the papilla which is considered of standard size. To achieve this, we implement a locating technique for finding and measuring the papilla on fundus images.

1 Introduction

Since the eye is considered an outgrowth of the brain, it is reasonable to assume that changes in the vasculature of the retina reflect changes in blood microcirculation of the brain. Hypertension, even at an early stage, is known to manifest itself in the retina by attenuation changes, focal narrowing and occlusion of retinal vessels. Automatic quantification of these changes would be a great step not only in the direction of diagnosis of hypertension, but also towards an optimised method for monitoring the progress of subsequent treatment.

The retinal vasculature can be considered a series of cylindrical pipes with respect to blood circulation [1]. The simplest hydrodynamic system is a long straight pipe with a steady flow through it. In such a pipe the head of the pressure (Δp) is directly proportional to the length (L), the flow (F), the viscosity of the fluid (μ) and inversely to the fourth power of the radius (R). This is the law of *Poiseuille*:

$$\Delta p = \frac{8 L \mu F}{\pi R^4}$$

It is therefore clear why the calibre of the vessel is important in any attempt to recognise the presence or progress of systemic hypertension. By injecting dye into retinal vessels and then studying the fluorescein angiograms it has been observed [1] that there are two distinct types of flow in the vessels, laminar and turbulent. Laminar flow can be regarded as a series of concentric laminae moving faster at the axis than away from it. When two pipes with such flow join, dye from one of them will not mix with the other and the two streams run side by side. As the rate of flow through the pipes increases there comes a point where mixing occurs and the regular lines of laminar flow are lost. The new type of flow is no longer governed by Poiseuille's law and is termed "turbulent". The breakdown of laminar flow depends upon the diameter of the tube (D),

the mean velocity of the flow (V), the density (ρ), and the viscosity (μ) of the fluid. The point of transition from laminar to turbulent flow depends upon the value of the Reynolds number (R_e), which is calculated as:

$$R_e = \frac{VD\rho}{\mu}$$

It should be noted that the critical value of the Reynolds number for any fluid (including blood) to become turbulent is about 2000 [1] and narrowing of the vessels alone has not been accepted as a sole reason for turbulence. Eddy formation along the walls is also mentioned as a possible culprit. However, it is established that transition to turbulence in retinal vessels always occurs close to bifurcations. This is why length to next bifurcation, as well as wall thickness are critical in the study of hypertension induced retinopathy. For a recent method of tracking and studying flow transitions see [2].

The first step in performing measurements of blood vessels is to extract the vessels from their background. Estimating the location of blood vessel boundaries within images of a living vascular network "has all the problems associated with image segmentation of biological data and still remains a difficult problem" [3]. This is largely because such images have low signal-to-noise ratio and limited spatial resolution. The algorithms proposed for tracing vessels and can be generally classified in three categories:

- model fitting, which identifies edge points by optimising a function fitting (*e.g. a Gaussian*) on the intensity profile of a vessel.
- optimal filtering, where gray level thresholds are specified based on the distribution of pixel properties (*e.g. adaptive thresholding*)
- sequential contour tracing, where active contour models (*e.g. "snakes"*) are used to perform a global region extraction

F.P. Miles and A.V. Nuttall [3] studying blood flow in the cochlea of the ear, proposed an algorithm that estimates diameter and position of vessels by minimising the mismatch between the measured intensity profile and a finite set of intensity profile models, thus constructing a matched filter estimator. A similar approach is adopted by Zhou *et al* in [4]. Here, the centerline is tracked using an adaptive densitometric technique to improve computational performance in regions where the vessel is relatively straight. Their method calculates vessel calibre and wall location (*but not vessel wall thickness*) as well as a curvature index defined as the ratio of the pixel length of the centerline over the distance between two points. This algorithm fails at arteriovenous crossings and no information is given on its behaviour in bifurcations. Initial centerline point and direction are expected to be given by the end user.

Alternatively, T. McInerney and D.Terzopoulos [5] have presented a topologically adaptable snakes model for angiogram segmentation. Their model benefits from reparametrization during the deformation process. Still, it suffers from the problem of initialisation common to snake models. The authors report that they had to perform the segmentation of the vascular network one branch at a time freezing the snake manually once it began to flow into a crossing branch. Similar user input is anticipated in the recent work of Klein *et al* [6].

2 Method Overview

All absolute measurements undertaken in fundus images are prone to errors caused by a number of reasons. Prominent among these reasons is the refraction of light from the lens of the eye as well as the liquid that fills the area between the cornea and the retina (*vitreous humor*). Other error inducing factors are visual impairments of the eye, i.e whether the eye is emmetropic or not, as well as the sharpness of the image. Littmann has presented a method for calculating these errors in [7] but his method and formulae have been critisized in [8] and [9] and more recently by Sanchez in [10]. To minimise the impact of such errors during our study, we calibrate all our measurements according to the size of the papilla which constitutes a reference feature for our images. In order to identify the papilla we used a disk fitting procedure that is explained in [11]. The estimate of our method had less than 2% deviation from the true radius measured explicitly (Fig. 1a).

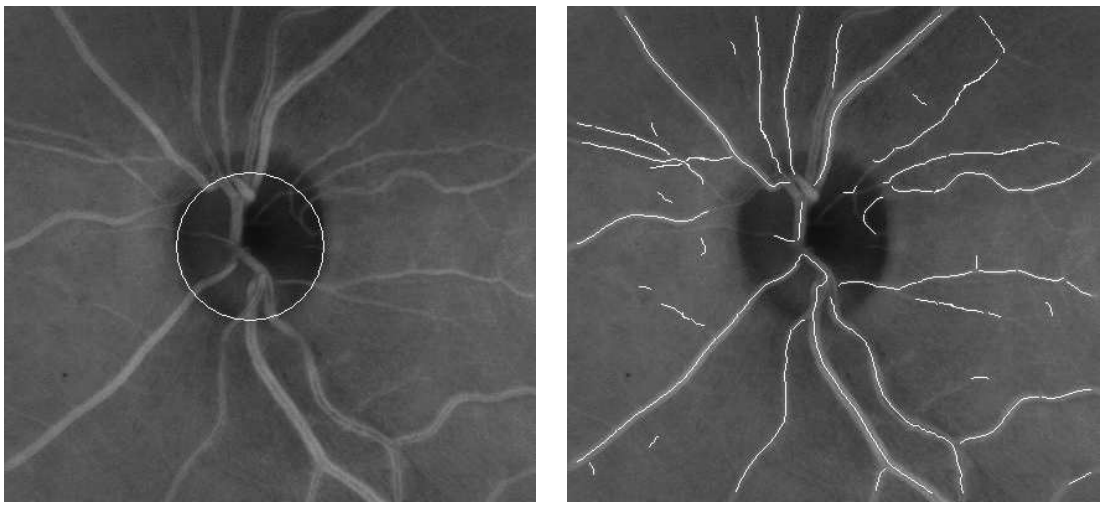

(a) (b)

Figure 1. (a) Papilla location on a fundus image (b) Tracked centerlines superimposed on raw data.

2.1 Ridge Detection

Ideally we would wish to obtain a pixel-wide line running through the centre of each vessel. This would greatly facilitate tracking the vessels and simplify our measurements. However, a cross-sectional intensity profile of a typical vessel (Fig. 2a,c) indicates that vessels present two peaks separated by a valley. This is due to the variation in intensity caused by the blood stream inside the vessel. To overcome this a gaussian smoothing is introduced (Fig 2b,d). Once the image is smoothed a directional map [11, 12] is being built by scanning the image and registering the direction of the gradient at each point. The image is scanned again and ridge points are identified by suppressing pixels which do not satisfy the following criteria:

- Directional consistency with their neighbouring pixels
- Intensity supremacy over their neighbouring pixels in the direction orthogonal to the tentative direction of the vessel
- Contrast maximization in the direction orthogonal to the tentative direction of the vessel

During the ridge point identification, the image is binarized and after that it undergoes a filtering process to clean some noise by removing individual pixels. Dilation and erosion cater for fragmented vessels. At this point thinning filters prepare the image for tracking. The vessels are then tracked and a list containing pixel co-ordinates is produced. A second filtering of vessels under a certain length practically eliminates noise completely and concludes the segmentation.

3 Measurements of Retinal Structures

In this section we present a possible use of the vessel extraction derived earlier in order to make estimates for sizes of retinal structures. We are mainly interested in the length of vessels until next bifurcation, the width of the vessel lumen (hereafter referred to as "vessel calibre") and the width of the wall of the vessel. We also introduce a measure of tortuosity for the vessels and present relevant calculations for our demonstration image.

3.1 Vessel length

We estimate the length of a vessel by consulting the tracked file and counting the pixels for each individual track. This approach is under the assumption that the length of the centerline is a good

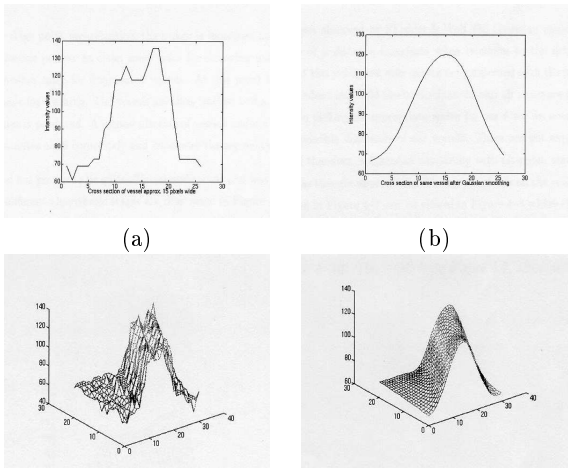

Figure 2. Vessel profiles before (a),(c) and after smoothing (b),(d)

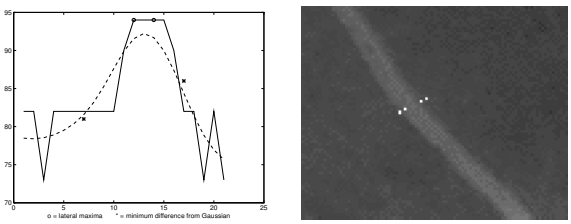

Figure 3. Application of the width estimation method on a vessel profile

approximation of the length of the vessel and that our tracker stops at bifurcations and gives a new track for every sub-vessel. We note that of medical interest in our case is not the *total* length of a vessel but the length until the next bifurcation. This allows for monitoring hypertensive retinopathy which makes vessels bifurcate earlier than they do in normatensive persons [13]. The length of the tracks is reported as the tracks are met in the track file. In Fig. 1b the tracks are simply overlaid on the original greyscale image. Other configurations that would enhance the visualisation of such results, such as colour-coding for short-bifurcating vessels, are possible.

3.2 Estimation of Vessel Calibre and Wall

Apart from the significance of the vessel calibre changes that lead to (and depend on) pressure fluctuations, it is apparent that the width of the wall is an interesting parameter in monitoring atherosclerotic changes that result from hypertension. Since at this point we have identified the pixel co-ordinates of the points that constitute the centerline at each vessel, we can use these to determine automatically the width.

We do this by first sampling the original image in a direction orthogonal to the local direction of the vessel. We also sample the same points from the smoothed image. Sampling goes out a set number of pixels to the "left" and to the "right" of the scanned pixel in a direction orthogonal to the local direction of the vessel. The rationale for doing this is that the points less affected by the Gaussian smoothing (in the region sampled) will be the ones that lie closer to the border of a blood vessel. Additionally we identify the two maxima to the left and to the right of each point registered in the tracked file. These are taken to correspond to the beginning of the lumen of the vessel in either side. In Fig. 3 we can see the application of our technique on a cross-sectional profile of a vessel that appears in our test image.

Once the co-ordinates of those pixels are stored, the width of the vessel at every point that has been recorded by the tracker can be estimated using, for example, the Euclidean distance between the two external pixels that have been calculated for this particular point. This way we can have a detailed width variation of each particular vessel along its length as well as an average width of all the vessels tracked. Also, we can easily estimate the wall width as the distance between the pixel where the sample from the original has a maximum and the respective pixel that was found to represent the wall on that side.

3.3 Tortuosity

We measure tortuosity by averaging the change of angle calculated at reasonable discrete steps along the length of the vessel. The change of angle is independent of scale and does not cancel out along the length of the vessel. We therefore introduce as *mean tortuosity index* of a track, T_t, a number derived in the following manner: for each pixel indicated in the track list, P, we consider two more centerline pixels, P-s and P+s that lie a set number of pixels behind and ahead of P, respectively. We then form the vectors (P-s,P) and (P,P+s) and we normalise them by dividing each with its norm. Lastly, we form their dot product and take the inverse cosine of this product. If we average these angles over the number of points used along the vessel track we get the mean tortuosity index of the respective track. This index is not reported when very few points are sampled (e.g ten or less). In mathematical notation, the ideas expressed above can be formulated as:

$$T_t = \frac{1}{(t_length - 2 * step)} * \sum_{n=step}^{(t_length-step)} \arccos(UV(P_{n-step}, P_n) \bullet UV(P_n, P_{n+step}))$$

where t_length stands for the length of the particular track and UV means unary vector. With this kind of tortuosity measure we can also have an idea of variation of tortuosity along a vessel. The format of the results we get is:

```
Track # 1  Average tortuosity N/A Very few points tested 1
........
Track # 21 Average tortuosity 0.1513 # points tested 120
.......
Track # 30 Average tortuosity 0.3418 # points tested 92
Track # 31 Average tortuosity N/A Very few points tested 7
Track # 32 Average tortuosity 0.3522 # points tested 38
........
```

In Fig. 4 we have numbered the tracks to indicate correspondence with results and we have removed the papilla region because vessels twist and bend a lot on the verge of coming out of the optic disk, hence we would have accepted false indications of tortuosity as true. Tracks 30 and 32 have a markedly higher index of tortuosity which is reasonable given that their curves are more sharp than, say, track 21.

4 Future work

The work presented here describes a method for evaluating the relationship between retinal findings and hypertension. In that sense, we feel that the ridge detection technique has proved ideal for our purposes and could well be used in an extension of this work into an integrated software tool in support of a physician's practise. The fact that this method can be applied on fluorescein-free fundus images facilitates frequent re-examination and monitoring of hypertensive patients. A possile future extension would be to work with coloured images. This way one could study standard arteriovenous indices such as artery to vein ratio, or arteriovenous crossings. A further step towards the integration of the presented techniques would be to form a grading scale on the severity of hypertension based on weighted numerical results from our method. Ideally, classification in this scale will be by the software itself either through the use of classic AI techniques, e.g. through an Expert System, or through a Connectionist approach where a Neural Network could be trained to

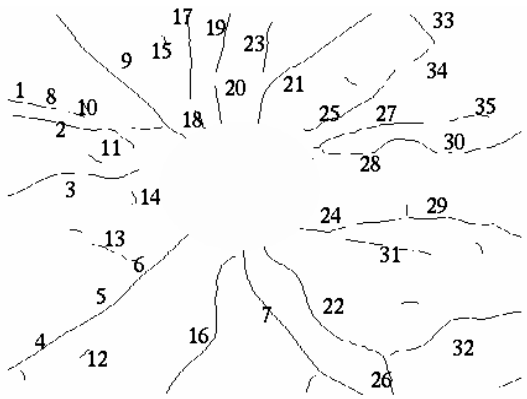

Figure 4. Some of the original tracks after the removal of the papilla region

recognise the hypertensive patient's symptoms. Such software should be able to connect directly, or through a custom interface, to a patients' database for consultation and maintenance.

Acknowledgements

This study was motivated by research undertaken in the Medical Renal Unit of the Royal Infirmary of Edinburgh with respect to hypertension. Dr. G. Kyriazopoulos, M.D., co-ordinated the experiments on behalf of the Renal Unit, while the researchers of the Machine Vision Unit at the Dept. of Artificial Intelligence, University of Edinburgh, gave critical insight in the design of the method.

References

[1] G Wise, Dollery C, and Henkind P. *The Retinal Circulation*. Harper and Row, 1971.

[2] D. Androutsos, P.E. Trahanias, and A.N. Venetsanopoulos. Application of active contours for photocromic tracer flow extraction. *IEEE Transactions on Medical Imaging*, 16(3):284–293, Jun 1997.

[3] FP. Miles and AL. Nuttal. Matched filter estimation of serial blood vessel diameters from video images. *IEEE Transactions on Medical Imaging*, 12(2):147–152, 1993.

[4] L Zhou, Rzeszotarski MS, Singerman LJ, and Chokreff JM. The detection and quantification of retinopathy using digital angiograms. *IEEE Transactions on Medical Imaging*, 13(4):619–626, 1994.

[5] T McInerney and Demetri Terzopoulos. Topologically adaptable snakes. In *IEEE International Conference on Computer Vision*, MIT, Boston, 1995.

[6] A.K. Klein, Forester Lee, and Amir A. Amini. Quantitative coronary angiography with deformable spline models. *IEEE Transactions on Medical Imaging*, 16(5):468–482, 1997.

[7] H. Littmann. Zur bestimmung der wahren grosse eines objektes auf dem hintergrund des lebenden auges. *Klin Monatbl Augenheilkd*, 180:226–289, 1982.

[8] AG Bennet, Rudnicka AR, and Edgar DR. Improvements on Littman's method of determining the size of retinal features by fundus photography. *Graefe's Arch Clin Exp Ophthalmol*, 232:361–367, 1994.

[9] P. Baumbach, Rassow B., and Wesserman W. Absolute fundus dimensions measured by multiple beam interference fringes. *Invest Opthalmology Vis Sci*, 30:2314–2330, 1989.

[10] A. Sanchez, J.M. Larrosa, and F.M. Honrubia. Improvements on Littman's theoretical method. *Graefe's Arch Clin Exp Ophthalmol*, 233(8), 1995.

[11] K.V. Chandrinos. Quantifying atherosclerotic changes with digital image processing. Master's thesis, Dept. of Artificial Intelligence, University of Edinburgh, 1995.

[12] R. Kutka and S. Stier. Extraction of line properties based on direction fields. *IEEE Transactions on Medical Imaging*, 15(1):51–58, Feb 1996.

[13] N.L. Stokoe. Arteriosclerosis and hypertension. In A.T. Proudfoot, editor, *The Eye in Medicine*, volume 49, pages 39–55. The Royal College of Physicians of Edinburgh, 1977.